

## SILVER ADDITIONS INFLUENCE ON BIOMEDICAL POROUS Ti-Ni SMAs FABRICATED BY MICROWAVE SINTERING

Mustafa K. Ibrahim<sup>a</sup>, E. Hamzah<sup>a\*</sup>, Safaa N. Saud<sup>b</sup>, E. M. Nazim<sup>a</sup>,  
Abdollah Bahador<sup>a</sup>

<sup>a</sup>Faculty of Mechanical Engineering, Universiti Teknologi Malaysia,  
81310 UTM Johor Bahru, Johor, Malaysia

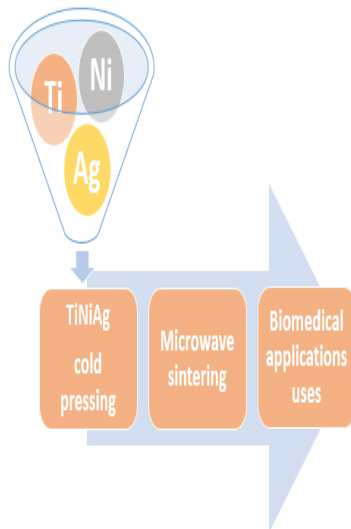
<sup>b</sup>Faculty of Information Sciences and Engineering, Management &  
Science University, Shah Alam, Selangor, Malaysia

### Article history

Received  
31 October 2017  
29 January 2018  
Accepted  
15 February 2018  
Published online  
3 June 2018

\*Corresponding author  
esah@fkm.utm.my

### Graphical abstract



### Abstract

Ti-Ni and Ti-Ni-Ag shape memory alloys (SMAs) were prepared by microwave sintering. In Ti (49 -%Ag)-Ni51-Ag (atomic percentage), the silver was added with three percentages of (0.246, 0.5 and 1.51) at. %, respectively. The influence of Ag addition on the microstructure, phase composition, transformation temperatures and mechanical properties were investigated by scanning electron microscopy (SEM), X-ray diffraction (XRD), differential scanning calorimeter (DSC) and compression test. The microstructure shows needles and plates inside Ti-rich region. The R phase appears at the plane (-112) and the plane (300). This phase has appeared during cooling and heating of the baseline of DSC test. The compression strain at maximum strength was improved, while the compression strength was reduced. The highest compressive strain was for the sample with 0.246 at. % Ag. The elastic modulus decreases with the increasing of Ag content. The elastic modulus of these alloys was low that make it proper for biomedical applications such as natural human bone due to the sintering method and also improve by adding silver.

**Keywords:** Biomedical Ti-Ni-Ag SMAs, Mechanical alloying, Microwave sintering, Microstructure, Mechanical properties

### Abstrak

Ti-Ni dan Ti-Ni-Ag membentuk memori aloi (SMA) yang disediakan oleh pensinteran gelombang macro. Dalam Ti (49 -% Ag) -Ni51-Ag (peratusan atom), perak telah ditambahkan pada tiga peratusan, masing-masing (0.246, 0.5 dan 1.51). Pengaruh penambahan Ag pada mikrostruktur, komposisi fasa, perubahan suhu dan sifat mekanik telah disiasat dengan mengimbas mikroskop elektron (SEM), pembelauan X-ray (XRD), perbezaan pengimbasan kalorimeter (DSC) dan ujian mampatan. mikrostruktur ditunjukkan oleh jarum dan plat di dalam kawasan Ti-Rich. Fasa R muncul pada tahap (-112) dan tahap (300). Fasa ini telah muncul semasa penyejukan dan pemanasan asas ujian DSC. Terikan mampatan pada kekuatan maksimum bertambah baik, manakala kekuatan mampatan dikurangkan. Terikan mampatan tertinggi adalah untuk sampel dengan 0,246 di. % Ag. Modulus elastik berkurangan dengan peningkatan kandungan Ag. Modulus elastik aloi ini adalah rendah yang menjadikannya sesuai untuk aplikasi bioperubatan seperti tulang manusia semula jadi kerana kaedah pembakarannya dan juga bertambah baik dengan menambahkan perak.

**Kata kunci:** Biomedical Ti-Ni-Ag SMA, pengalioian mekanikal, Microwave pembakaran, mikrostruktur, sifat-sifat mekanikal

© 2018 Penerbit UTM Press. All rights reserved

## 1.0 INTRODUCTION

Ti-Ni based SMAs are important biomaterials due to the good engineering properties including biocompatibility, shape memory effect (SME) and superelasticity. The applications of Ti-Ni SMAs have been spread to the medical field, aerospace, and aviation, etc. [1-3]. TiNi alloys have been widely applied as biomaterials in implant devices and making biomedical apparatus, due to their good biological properties and biocompatibility as well as their unique superelasticity and shape memory effects [4]. Porous Ti-Ni alloys have attracted more interest for bio implantation since the presence of the pores in the bulk material improves the growth of body tissues, reduces the alloy density and corporate fixation [5]. Therefore, alternative processing routes that have the ability to control grain size and composition, such as mechanical alloying and powder metallurgy (PM) as fabrication processes were developed [6, 7]. These processes are solid-state powder techniques that are widely used to produce refractory metals, dispersion-strengthen alloys, nanocrystalline, and amorphous composite materials [8-10]. A number of researchers have studied the transformation characteristics of Ti-based produced by PM, and then sintered using different kinds of sintering techniques [11-14]. Most of these techniques have disadvantages, including being time-consuming, the presence of a high percentage of porosity/cracks, and thus the reduction in the mechanical properties. Microwave sintering involves a new sintering routine used to heat the green compacts nearly to a sintering temperature for densifying and alloying the metals, ceramics, and composites. It is able to incorporate the pre-alloyed elements using microwaves and volumetrically absorb the electromagnetic energy, and then transform it into heat [15-17]. In contrast to the typical sintering methods, the microwave sintering approach demonstrates several fundamental features, minimized energy intake, rapid heating rates, minimized sintering times, improved element diffusion processes, and enhanced physical and mechanical properties [15].

Powder metallurgy is a promising method for producing of porous near-net-shape components [18, 19]. The only limitation is the occurrence of the lower elastic modulus (although higher than that of bone) of Ti-based alloys than many others. Consequently, achieving lower elastic modulus (Young's modulus) requires certain efforts in the design steps where the elastic modulus should be reduced concurrently with the thermo-elastic behavior of these alloys. In this research, the steps of reducing the elastic modulus will be depending on the sintering method and adding Ag element. It is reported that adding Ag improves the corrosion resistance and antibacterial properties of the titanium [20, 21]. Therefore the main aim in this research to study the effect of Ag additions on

microstructure and mechanical properties of Ti-Ni SMAs.

## 2.0 METHODOLOGY

The materials (Ti, Ni and Ag) were supplied by Stanford Advanced Materials Company, USA. The silver was added In Ti-Ni-Ag SMAs with three percentages of (0.246, 0.5 and 1.51) at. %, respectively, silver additions to Ti-Ni SMA of small percentages due to the cytotoxicity of Ag [22]. Titanium of particles size 150  $\mu\text{m}$  and purity (99.5%) mixed with nickel of particles size 45  $\mu\text{m}$  and purity (99.5+ %) and silver of particles size 45  $\mu\text{m}$  for 1 h in a planetary ball mill (PM100, made in Germany) at a speed of 300 rpm and ball to powder weight ratio of 4:1. Ti (49 -%Ag) -Ni51-Ag powders were cold-pressed to green samples of ( $\Phi 25 \times 10$ ) mm under a uniaxial pressure of 230 kg/cm<sup>2</sup> for 5 min, followed by microwave sintering (MWS), MWS machine type (HAMiLab-V3, SYNOTHERM Corp, manufacturer China). These samples were MWSed at a temperature of 700 °C for 15 min at a heating rate of 30 °C/min. Then, these samples were machined to dimensions of (7 mm  $\times$  7 mm  $\times$  14 mm) by using electrical discharge machining (EDM) CNC wire cut machine (Sodick, AQ 537L, made in Japan) for a compression test, according to the standards of (ASTM E9-09). These samples were coupled with microwaves which were absorbed electromagnetic energy and transformed them to heat to adjust the sintering temperature. Figure 1 shows MWS insulation barrel was set up into continuously a 2.45 GHz and 4.5 kV. The sintering was under argon gas fills the sintering chamber with gas flow purity of (99.999%). The compacts were placed in alumina crucible surrounded by silicon carbide (SiC) particles (at the corners of the alumina crucible). Silicon carbide uses as auxiliary heat material. The Infrared pyrometer uses to measure the temperature of the samples during sintering.

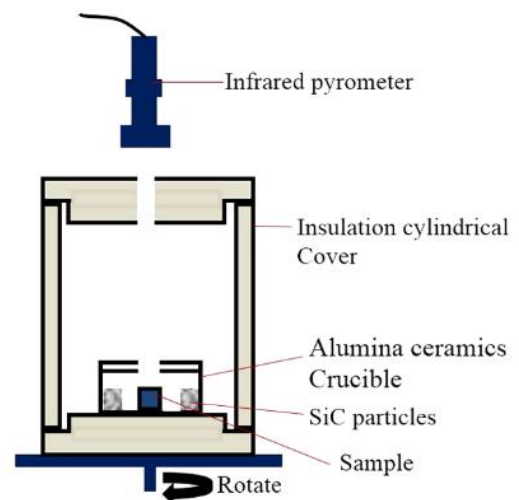


Figure 1 Shows MWS insulation barrel

The relative density was tested by the Archimedes drainage method. Scanning electron microscopy (SEM, Hitachi Model S-3400N, made in Japan) was used to analyze the microstructure (at magnification 2500x), as well the composition via the energy dispersive spectroscopy (EDS). The X-Ray diffractometer (XRD, D5000 Siemens, made in Germany) was used to characterize the phase composition of Ti-51%Ni-Ag samples, the planes of the phase composition were identified by the jade software. The XRD used a CuK $\alpha$  X-ray source, and the scanning mode was locked couple with a scan rate of 0.05°/sec and a 2 $\theta$  range between 20°C to 90°C. The differential scanning calorimeter (DSC Q200, TA Instrument manufacturer in New Castle, Delaware) was used to identify the phase transformation temperatures of these alloys using TA Instrument software under heating /cooling rates of 10 °C/min. Instron 600 DX-type universal (Industrial equipment supplier in Singapore) testing machine was used to perform the compression test at a constant speed of 0.5 mm/min at 25 °C.

### 3.0 RESULTS AND DISCUSSION

#### 3.1 Microstructure Characterization

The relative density of Ti-Ni and Ti-Ni-Ag was in a very small range between (81%-82%) due to the sintering parameters of temperature and time, the sintering temperature was 700 °C less than Ag element melting temperature (961.93 °C), with a short sintering time of 15 minute. The microstructure in Figure 2 shows Ti-rich and Ni-rich regions, and between those two regions the Ti<sub>2</sub>Ni, NiTi and Ni<sub>3</sub>Ti phases. The Ti-rich region contains on plates-like and needles-like microstructure morphologies. Figure 2 displays the microstructure of Ti-Ni and Ti-Ni-Ag including the regions which appeared and the influence of Ag additions on the microstructure. The EDS shows Ag diffusion toward Ni-rich region more than the diffusion toward Ti-rich region.

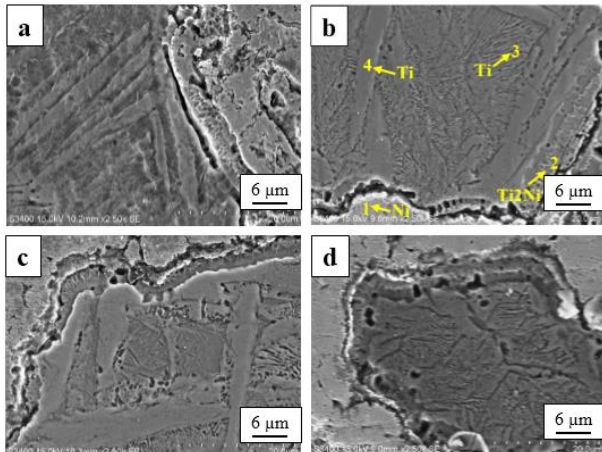


**Figure 2** SEM micrographs of Ti-51%Ni-Ag at (a) 0 at. %Ag, (b) 0.246 at. %Ag, (c) 0.5 at. %Ag, and (d) 1.51 at. %Ag

Figure 3 displays the energy dispersive spectroscopy (EDS) of Ti-51%Ni-0.246%Ag, (1-4) refers to the EDS points on a micrograph of Figure 2 (b). The presence of Ag element more in Ni-rich region than Ti-rich region. Figure 3 (1) shows the Ni-rich region with 88.47 at. % of Ni, Figure 3 (2) shows Ti<sub>2</sub>Ni phase region, while Figure 3 (3) shows Ti-rich region with 98.76 at. %Ti and Figure 3 (4) shows Ti rich region with 100 at. %Ti.

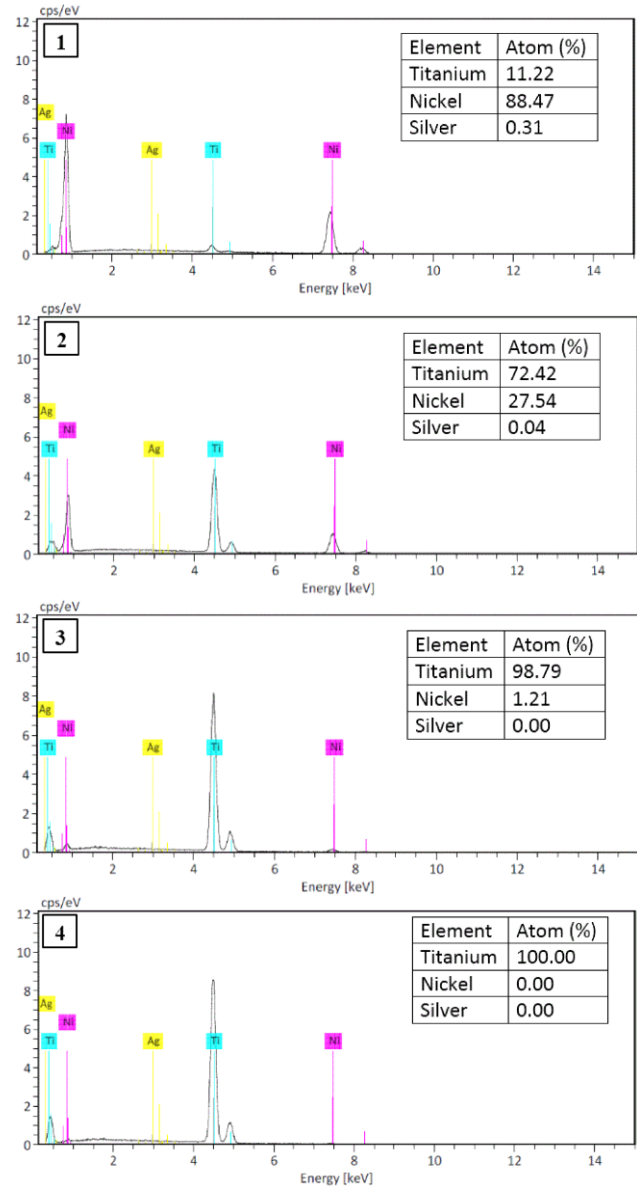


**Figure 3** EDS of Ti-51%Ni-0.246%Ag, (1-4) refers to the EDS points on the micrograph of Figure 2 (b), ■ Ti, ■ Ni and ■ Ag

Figure 4 shows XRD patterns of microwave-sintered Ti-Ni-Ag. These alloys are showing  $\beta_2$  (NiTi),  $\beta_{19}$  (NiTi), Ni<sub>3</sub>Ti, and Ti<sub>2</sub>Ni. The  $\beta_2$  phase appears at the plane (110) of the angles 35.2 and 38.38°, (200) of the angle 51.7° and the plane (220) of the angle 76°. The  $\beta_{19}$  phase appears at the planes (002), (111), (020) and (111) of the angles 40.2°, 41.45°, 43.63°, and 44.48°, respectively. While the Ti<sub>2</sub>Ni phase appears at

the planes (511), (440) and (660) of the angles  $41.45^\circ$ ,  $45.4^\circ$ , and  $70.6^\circ$ . Ni<sub>3</sub>Ti phase appears at the planes (201), (004), (202), (203) and (220) of the angles  $42.36^\circ$ ,  $43.63^\circ$ ,  $46.5^\circ$ ,  $53^\circ$  and  $74^\circ$  [23]. The R phase appears at the plane (-112) of the angle  $53^\circ$  and the plane (300) of the angle  $71.5^\circ$ . The intensities of several peaks were increased with increasing Ag additions.

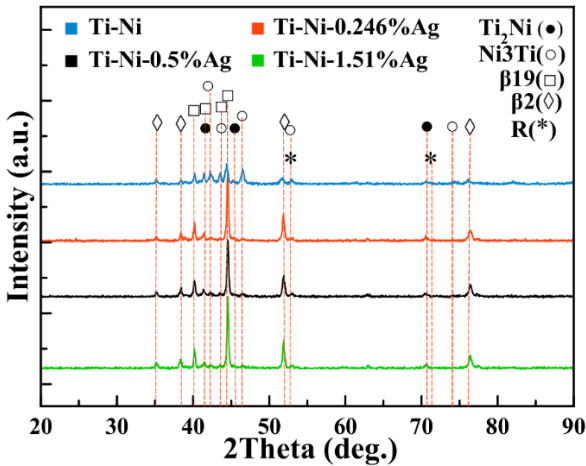


**Figure 4** XRD of Ti-Ni and Ti-Ni-Ag samples sintered at  $700^\circ\text{C}$  for 15 min

### 3.2 Transformation Temperatures

Figure 5 displays differential scanning calorimeter (DSC) curves of Ti-51%Ni-Ag SMAs. The transformation temperatures of these SMAs were determined by TA Instrument software accompanying the DSC instrument. The transformation temperatures, austenite start and martensite start ( $A_s$  and  $M_s$ ) temperatures, and austenite finish and martensite finish ( $A_f$  and  $M_f$ ) temperatures were identified by the conventionally employed extrapolation of the temperatures of the onset and offset on the curve baseline (See Table 1); utilizing the extrapolating temperatures of the onset and offset in the thermal analysis is common. The utilization of deviation point from the curve baseline (onset and offset temperatures) might have been better instead of extrapolating temperatures to explain the strange influences in the DSC curves of diffusionless martensitic transformations. Therefore, an extrapolating value was used to satisfy the universal trend in the DSC and prevent the subjectiveness of the selection of deviation point. A multi-step phase transformation in which  $\beta_{19}$  transforms to R, R transforms to  $\beta_2$  is observed during heating. The presence of R phase during heating of Ti-Ni SMAs was reported by earlier studies [24–26]. While during heating  $\beta_{19}$  transforms to R and R transforms to  $\beta_2$ .

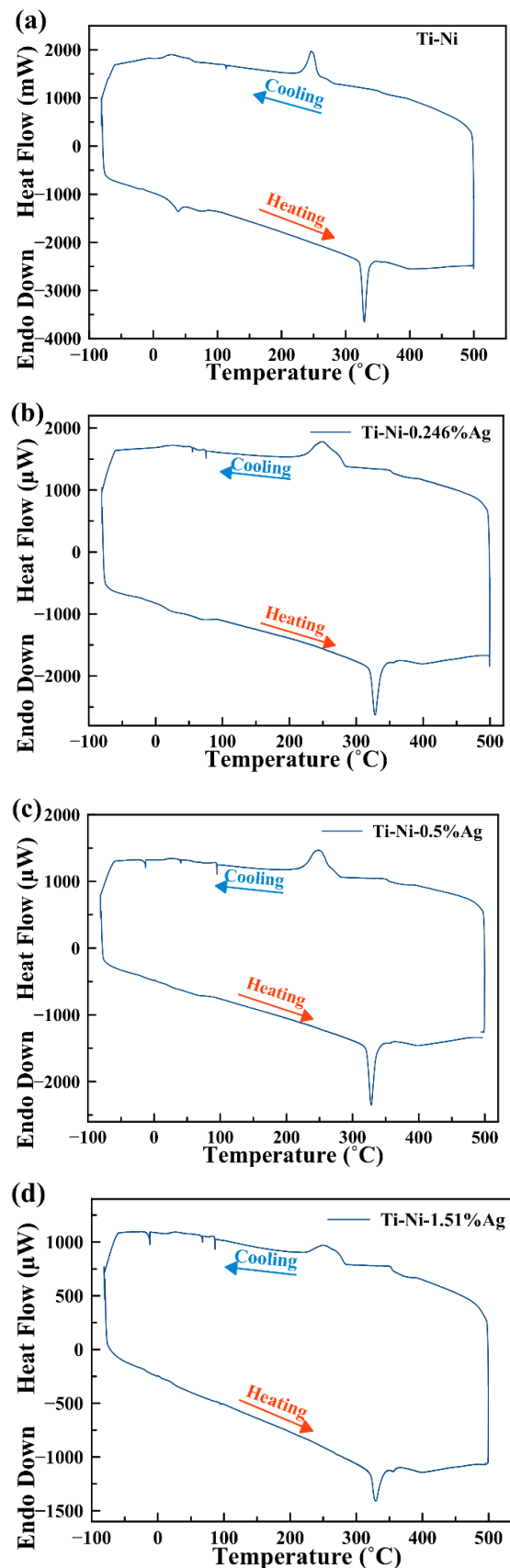


**Figure 5** Differential scanning calorimeter (DSC) curves of the Ti-Ni-Ag samples at (a) 0 at. %Ag, (b) 0.246 at. %Ag, (c) 0.5 at. %Ag, and (d) 1.51 at. %Ag

Table 1 Transformation temperatures

| Ti-Ni-Ag alloys | Rs (°C) during cooling | Rf (°C) during cooling | Ms (°C) | Mf (°C) | Rs (°C) during heating | Rf (°C) during heating | As (°C) | Af (°C) |
|-----------------|------------------------|------------------------|---------|---------|------------------------|------------------------|---------|---------|
| Ti-Ni-0%Ag      | 282.5                  | 231                    | 65      | 10.1    | 25.7                   | 88                     | 319     | 338     |
| Ti-Ni-0.246%Ag  | 357                    | 217                    | 44.7    | 1       | 4.7                    | 90.5                   | 319     | 360     |
| Ti-Ni-0.5%Ag    | 355                    | 221                    | 61      | 13.6    | 17.6                   | 80                     | 318.5   | 359.9   |
| Ti-Ni-1.51%Ag   | 357                    | 220                    | 37      | 14.5    | 18                     | 86                     | 320     | 362     |

### 3.3 Mechanical Properties (Stress-Strain Curves)

Figure 6 displays the effect of silver content on the stress-strain curves of Ti-Ni-Ag. The maximum strain was improved with increasing of the silver, but in the same time the maximum strength was reduced. The Ag element was reduced the elastic modulus. The elastic modulus value of (0, 0.246, 0.5, and 1.51) at. % Ag samples were (14.28, 11.1, 11, and 7.5) GPa, respectively. The elastic modulus reduces gradually with the increasing the amount of Ag. However, the "stress shielding" term considers one of the most critical issues frequently encountered in hard tissue replacement applications is generated from the large difference in the hard tissue elastic modulus of (<20 GPa) and the implant materials elastic modulus of (>100 GPa), which may lead to the resorption of the hard tissue, loosening of the implants and finally, the failure of implantation [27-29]. These alloys are appropriate for the applications which required low elastic modulus such as human bone due to reducing of elastic modulus by adding silver and microwave sintering technique. The maximum compression strength of (0, 0.246, 0.5, and 1.51) at. % Ag samples were (580, 422, 401, and 322) MPa, respectively, while the maximum strain at these strengths was (5.3%, 12.47%, 11.8%, and 9.8%).

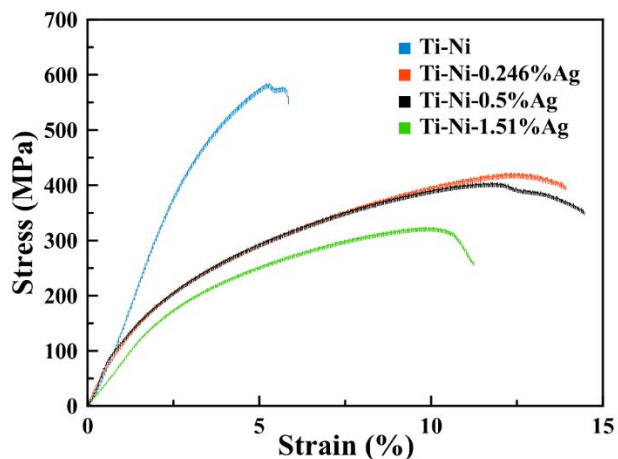


Figure 6 Compression test of Ti-Ni-Ag with different amount of the Ag element

## 4.0 CONCLUSION

The B2→R→B19' transformation was appeared during heating and cooling. The microstructure displays plates surround needles within the titanium-rich region. The increasing of silver reduces the elastic modulus and increasing the maximum strain of Ti-Ni-Ag alloys. The reducing of elastic modulus makes Ti-Ni-Ag more appropriate for biomedical uses.

## Acknowledgement

The authors would like to thank the Ministry of Higher Education of Malaysia and Universiti Teknologi Malaysia for providing the financial support under the University Research Grant No. Q.J130000.2524.12H60 and research facilities.

## References

- [1] Hwang, C., Meichle, M., Salamon, M. and Wayman, C. 1983. Transformation Behaviour of a Ti50Ni47Fe3 Alloy II. Subsequent Premartensitic Behaviour and the Commensurate Phase. *Philosophical Magazine A*. 47(1): 31-62.
- [2] Eckelmeyer, K. 1976. The Effect of Alloying on the Shape Memory Phenomenon in Nitinol. *Scripta Metallurgica*. 10(8): 667-672.
- [3] Liu, F., Ding, Z., Li, Y. and Xu, H. 2005. Phase Transformation Behaviors and Mechanical Properties of TiNiMo Shape Memory Alloys. *Intermetallics*. 13(3): 357-360.
- [4] Breme, H. and Helsen, J. 1998. Selection of Materials. *Materials as Biomaterials*. 471(96935): 4.
- [5] Itin, V., Gyunter, V., Shabalovskaya, S. and Sachdeva, R. 1994. Mechanical Properties and Shape Memory of Porous Nitinol. *Materials Characterization*. 32(3): 179-187.
- [6] S. M. Tang, C. Y. C. a. W. L. 1997. Preparation of Cu-Al-Ni-based Shape Memory Alloys by Mechanical Alloying and Powder Metallurgy Method. *Journal of Materials Processing Technology*. 63: 307-312.
- [7] Ibarra, A., Juan, J. S., Bocanegra, E. H. and Nó, M. L. 2006. Thermo-mechanical Characterization of Cu-Al-Ni Shape Memory Alloys Elaborated by Powder Metallurgy. *Materials Science and Engineering: A*. 438-440: 782-786.
- [8] Suryanarayana, C. 2001. Mechanical Alloying and Milling. *Progress in Materials Science*. 46(1-2): 1-184.
- [9] Lu, W., Yang, L., Yan, B., Huang, W.-h. and Lu, B. 2006. Nanocrystalline Fe84Nb7B9 Alloys Prepared by Mechanical Alloying and Ultra-High-Pressure Consolidation. *Journal of Alloys and Compounds*. 413(1-2): 85-89.
- [10] Manna, I., Chattopadhyay, P. P., Banhart, F. and Fecht, H. J. 2004. Solid State Synthesis of Amorphous and/or Nanocrystalline Al40Zr40Si20 alloy by Mechanical Alloying. *Materials Letters*. 58(3-4): 403-407.
- [11] Pourkhorshidi, S., Parvin, N., Kenevisi, M., Naeimi, M. and Khaniki, H. E. 2012. A Study on the Microstructure and Properties of Cu-based Shape Memory Alloy Produced by Hot Extrusion of Mechanically Alloyed Powders. *Materials Science and Engineering: A*. 556: 658-663.
- [12] Vajpai, S., Dube, R. and Sangal, S. 2013. Application of Rapid Solidification Powder Metallurgy Processing to Prepare Cu-Al-Ni High Temperature Shape Memory Alloy Strips with High Strength and High Ductility. *Materials Science and Engineering: A*. 570: 32-42.
- [13] Vajpai, S. K., Dube, R. K. and Sangal, S. 2011. Microstructure and Properties of Cu-Al-Ni Shape Memory

- Alloy Strips Prepared via Hot Densification Rolling of Argon Atomized Powder Preforms. *Materials Science and Engineering: A*. 529: 378-387.
- [14] Portier, R. A., Ochin, P., Pasko, A., Monastyrsky, G. E., Gilchuk, A. V., Kolomytsev, V. I. and Koval, Y. N. 2013. Spark Plasma Sintering of Cu–Al–Ni Shape Memory Alloy. *Journal of Alloys and Compounds*. 577: S472-S477.
- [15] Oghbaei, M. and Mirzaee, O. 2010. Microwave Versus Conventional Sintering: A Review of Fundamentals, Advantages And Applications. *Journal of Alloys and Compounds*. 494(1-2): 175-189.
- [16] Das, S., Mukhopadhyay, A. K., Datta, S. and Basu, D. 2009. Prospects of Microwave Processing: An Overview. *Bulletin of Materials Science*. 32(1): 1-13.
- [17] Xu, J., Bao, L., Liu, A., Jin, X., Luo, J., Zhong, Z. and Zheng, Y. 2015. Effect of Pore Sizes on the Microstructure and Properties of the Biomedical Porous NiTi Alloys Prepared by Microwave Sintering. *Journal of Alloys and Compounds*. 645: 137-142.
- [18] Zhao, Y., Taya, M., Kang, Y. and Kawasaki, A. 2005. Compression Behavior of Porous NiTi Shape Memory Alloy. *Acta Materialia*. 53(2): 337-343.
- [19] Wu, S., Liu, X., Chu, P., Chung, C., Chu, C. and Yeung, K. 2008. Phase Transformation Behavior of Porous NiTi Alloys Fabricated by Capsule-free Hot Isostatic Pressing. *Journal of Alloys and Compounds*. 449(1): 139-143.
- [20] Chen, M., Zhang, E., & Zhang, L. 2016. Microstructure, Mechanical Properties, Bio-corrosion Properties and Antibacterial Properties of Ti–Ag Sintered Alloys. *Materials Science and Engineering: C*. 62: 350-360.
- [21] Li, W. R., Xie, X. B., Shi, Q. S., Zeng, H. Y., You-Sheng, O. Y., & Chen, Y. B. 2010. Antibacterial Activity and Mechanism of Silver Nanoparticles on Escherichia coli. *Applied Microbiology and Biotechnology*. 85(4): 1115-1122.
- [22] Biesiekierski, A., Wang, J., Gepreel, M. A. H., & Wen, C. 2012. A New Look at Biomedical Ti-based Shape Memory Alloys. *Acta Biomaterialia*. 8(5): 1661-1669.
- [23] Liu, A., Gao, Z., Gao, L., Cai, W. and Wu, Y. 2007. Effect of Dy Addition on the Microstructure and Martensitic Transformation of a Ni-rich TiNi Shape Memory Alloy. *Journal of Alloys and Compounds*. 437(1): 339-343.
- [24] Mentz, J., Frenzel, J., Wagner, M. F.-X., Neuking, K., Eggeler, G., Buchkremer, H. P. and Stöver, D. 2008. Powder Metallurgical Processing of NiTi Shape Memory Alloys with Elevated Transformation Temperatures. *Materials Science and Engineering: A*. 491(1): 270-278.
- [25] Yuan, B., Zhang, X., Chung, C. and Zhu, M. 2006. The Effect of Porosity on Phase Transformation Behavior of Porous Ti–50.8 at.% Ni Shape Memory Alloys Prepared by Capsule-Free Hot Isostatic Pressing. *Materials Science and Engineering: A*. 438: 585-588.
- [26] Su, P. and Wu, S. 2004. The Four-step Multiple Stage Transformation in Deformed and Annealed Ti 49 Ni 51 Shape Memory Alloy. *Acta Materialia*. 52(5): 1117-1122.
- [27] Geetha, M., Singh, A., Asokamani, R. and Gogia, A. 2009. Ti based Biomaterials, The Ultimate Choice for Orthopaedic Implants—A Review. *Progress in Materials Science*. 54(3): 397-425.
- [28] Nagels, J., Stokdijk, M. and Rozing, P. M. 2003. Stress Shielding and Bone Resorption in Shoulder Arthroplasty. *Journal of Shoulder and Elbow Surgery*. 12(1): 35-39.
- [29] Niinomi, M. 2008. Metallic Biomaterials. *Journal of Artificial Organs*. 11(3): 105-110.